Journal of Hydroscience and Hydraulic Engineering
Vol. 21, No.2 November, 2003, 47-59

AN EXPERIMENTAL STUDY ON DNAPL FINGERING MECHANISM IN SATURATED POROUS MEDIA

By

Takayuki Ueno
Technical Research Institute, Obayashi Corporation,
640, Shimokiyoto 4-chome, Kiyose-shi, 204-8558, Tokyo, Japan

Rabindra Raj Giri
Geosphere Research Institute, Saitama University,
255 Shimo-okubo, Sakura-ku, Saitama-shi, 338-8570, Japan

Kenji Nishida
Technical Research Institute, Obayashi Corporation,
640, Shimokiyoto 4-chome, Kiyose-shi, 204-8558, Tokyo, Japan

and

Kuniaki Sato
Geosphere Research Institute, Saitama University,
255 Shimo-okubo, Sakura-ku, Saitama-shi, 338-8570, Japan

SYNOPSIS

Knowledge of dense non-aqueous phase liquid (DNAPL) fingering phenomena in water-saturated porous media, which has not been investigated thoroughly, can be useful in gaining deeper insight into the contaminant transport and remediation. Laboratory experiments on fingering behaviors of trichloroethylene (TCE) through saturated porous media, randomly packed with uniform glass spheres in transparent glass box, were carried out. A basic mathematical model was developed and the experimental data on TCE fingering were interpreted based on it. The fingers grew almost linearly with time. The effective porosity of the media n_e with three kind sizes of glass sphere (d = 1, 2 and 3-mm) were between 4.0×10^{-2} and 5.0×10^{-2} irrespective of glass sphere size, while their invasion factor k_r increased with pore size. Numerical values of k_r varied from 5.0×10^{-4} to 5.0×10^{-2} in this study. TCE mobility and other fingering characteristics were evaluated by using Zhang and Smith's mobile-immobile-zone (MIZ) model. Findings showed that core diameter δ_c of the fingers were almost the same while size of immobile zone δ_f increased with finger Reynolds number Re and relative intrinsic permeability K_{rd}, which suggested that TCE with smaller mobility occupied wider pore space in the media. Values of Re in this study were in between 4.0 and 110.0. Thus, in this study we will deal with the difficulties of the fingering phenomenon.

INTRODUCTION

Dense non-aqueous phase liquids (DNAPLs), such as trichloroethylene (TCE) and perchloroethylene (PCE), are among the most frequently detected contaminants in the subsurface (Salah Jellali et al., 2001). Physical properties of DNAPLs are as follows: low viscosity, high density, low interfacial tension with liquid water, low absorbability to soil materials and low biodegradability. These properties make them highly mobile as well as persistent in the subsurface environment (Cohen and Mercer, 1993; Pankow and Cherry, 1996).

Once released into the saturated subsurface, DNAPL migrates downwards through the pores as a result of flow instabilities induced by viscosity and density differences between liquid water and DNAPL. The displacing instabilities at the interface produce finger like appearance of the migrating

DNAPL even in homogeneous saturated porous media (Held et al., 1995). This phenomenon is known as fingering. In real site contamination, remediation techniques and their efficiency are often limited by a lack of knowledge of DNAPL movement behavior (Salah Jellali et al., 2001). Fingering is one of the important transport mechanisms for non-aqueous phase transport in saturated subsurface. Therefore, it is essential to have thorough a knowledge of DNAPL fingering mechanism and its behavior for effective remediation of the contaminated sites.

Many researchers have been involved in clarifying DNAPL fingering mechanism in saturated porous media by both laboratory and field scale experiments. Most of the authors have pointed out the instability at the interface of the immiscible fluids as the primary reason for fingering (Kueper et al., 1988; Held et al., 1995; Zhang Yuyong et al., 2000; Oostrom et al., 1999). Held et al. (1988) investigated DNAPL migration in water saturated, homogeneous porous media using three-dimensional spill experiments. Their results showed that generation of finger pattern is sensitive to the porous medium grain size, DNAPL properties and spill conditions. Glass et al. (2000) experimentally demonstrated gravity-destabilized nonwetting phase invasion and existence of pulsation behind the invasion through a saturated heterogeneous porous medium. Zhang Yuyong et al. (2000) applied an approach based on invasion potential in pressure gradient to describe DNAPL displacement patterns under the influence of gravity. Oostrom et al. (1999) visualized non-aqueous phase TCE fingering through a saturated layered soil column using an intermediate-scale flow box experiment. The results showed that the fingers were relatively thin at fiest, and their movement and shape depended on porous media characteristics.

More specified investigations of DNAPL fingering have been conducted in the past few years. Smith and Zhang (2001) presented a modified method to determine effective interfacial tension of PCE penetration through a water-saturated porous medium and to predict finger wavelength (spacing). They observed another characteristic of fingering, which is termed as "tip-growing", in addition to tip-splitting, coalescing, and shielding. Zhang and Smith (2001) proposed a conceptual mobile-immobile-zone (MIZ) model to describe the structure of a DNAPL finger and velocity of finger propagation in the porous media, and experimentally verified the modeled prediction utilizing image analyses technique. The results showed that the fingers grow linearly with time, and that their lateral growth is insignificant once the tip of the finger passes a point of consideration. In another experimental investigation, Zhang and Smith (2002) concluded that use of classic equations on the basis of multiphase flow models without considering fingering phenomenon overestimates the averaged DNAPL content and underestimates the depth of DNAPL penetration.

Although many research works have been conducted on DNAPL fingering to date, the fingering mechanism has not yet been well understood and formulated. Therefore, there remains a challenge to scientists and researchers to thoroughly understand DNAPL fingering, which would be valuable in performing effective remediation of contaminated sites.

This paper aims to get gain a deeper insight into the DNAPL fingering mechanism in water-saturated porous media in two-dimensional laboratory scale experiments. The main objectives are: (a) to visualize DNAPL fingering process, (b) to describe and analyze the fingering mechanism, and (c) to predict finger dimension and velocity. The porous media in the experiments consisted of a two-dimensional box packed with uniform-size glass spheres, and dyed TCE was used as a typical DNAPL.

EXPERIMENTAL SETUP AND METHOD

Experimental Setup

Figure 1 shows a photographic view of the experimental setup. The components of the setup are ①: porous medium model, ②: microscope camera, ③: microscope body, ④: video monitor, and ⑤: video recorder, as indicated in the figure. DNAPL fingering in water-saturated porous medium models is recorded by means of a microscopic camera with high accuracy. The recorded pictures are digitized with the microscope body. The DNAPL fingering is displayed on the video monitor, and it is simultaneously recorded with video recorder. All the data are processed by an analyzer and a computer.

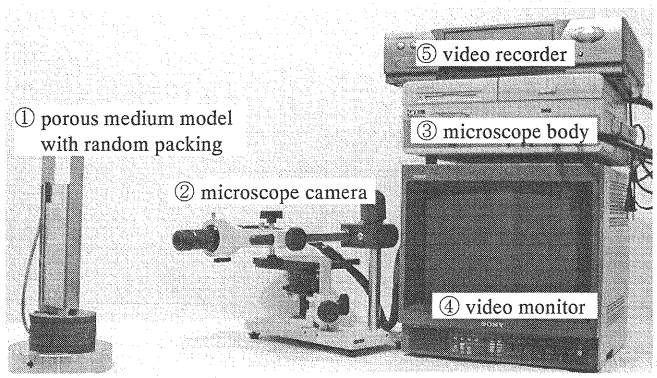

Fig. 1 A photographic view of experimental setup

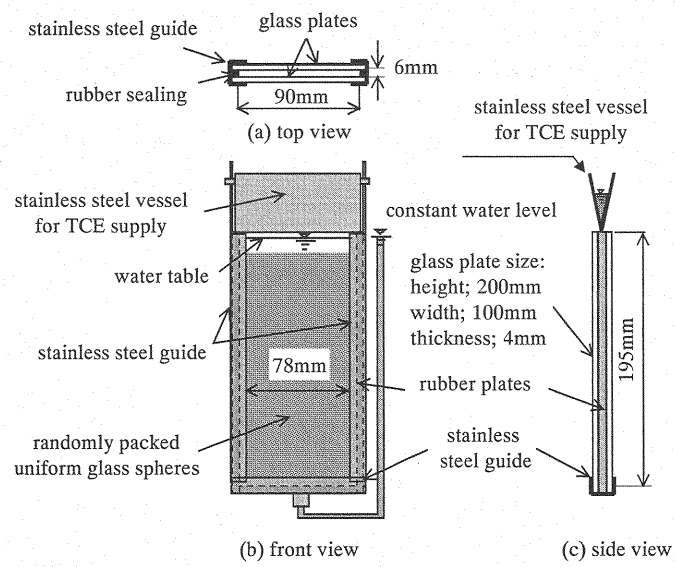

Fig. 2 A schematic diagram of porous medium

Porous Medium Models

A schematic diagram of the porous medium models used in the experiment is presented in **Fig. 2**. The models consist of a rectangular transparent glass box with 200-mm height, 100-mm width, and 6-mm thickness. The edge of the glass box is equipped with stainless steel guides and a completely seal for any leakage. The box is filled with uniform size glass spheres in random packing. Three kind sizes of glass sphere are employed in the experiments, as shown in **Table 1**. A constant head water pipe originates from the bottom of the box and extended up to its top, as shown in **Fig. 2**. A cone shaped stainless steel vessel is placed at the top of the box for non-aqueous phase TCE supply. TCE is dyed red with scarlet color for better visibility of finger images.

Experimental Procedure

The glass box is completely filled with water after clamping it vertical. Glass spheres are then placed into the box carefully in random packing, avoiding air bubbles within the box. About a 5-cm gap is maintained between the top surface of the glass spheres and water level, as shown in **Fig. 2**.

Table. 1 Experimental cases

glass sphere diameter (d) mm	porosity (n)	size of porous medium model (mm)			penetrating DNAPL
		width	height	thickness	
1.0	0.486	90	195	6	TCE
2.0	0.481				
3.0	0.537				

A known volume of dyed TCE is filled into the conical vessel and it is, then, placed over the box so that the tip of the vessel completely immerse into the water. The bottom valve of the conical vessel is gradually opened to pour TCE uniformly throughout the box cross-section. The cumulative volume of TCE poured into the box until the TCE just started to penetrate into the water-saturated pores is recorded. The recorded TCE volume divided by cross-sectional area of the box (90mm × 6mm) give an approximate pounding depth when TCE just started to penetrate. It is known as critical depth and denoted with h_{oc} (see **Fig. 3**). The TCE penetration is recorded using a video camera and video recorder set and are simultaneously displayed in the monitor. The process is continued until the finger reaches to the bottom of the box. The same procedure is repeated with other sets of porous media with three kind sizes of glass sphere. As shown in **Fig. 6**, the actual length of a finger ζ_s and its vertical projection ζ are measured from digitized pictures recorded in the experiments. The slopes of the lines obtained by plotting actual finger length and its vertical projection with time are taken as actual finger velocity w_s and vertical finger velocity w, respectively.

EXPERIMENTAL RESULTS

Transient TCE fingering at various points through a water-saturated porous medium model with 1-mm glass sphere size is presented as an example in **Fig. 3**. The critical pounding depth h_{oc} in this case is 2.1 cm, while the vertical distance traveled by the finger at 63 seconds is about 12.0 cm. The fingers for 2-mm and 3-mm glass sphere sizes are shown in **Fig. 4** (a) and (b). The critical pounding depths h_{0c} for 2mm is 1.8 cm, while the vertical distance ζ (t = 41sec) covered by fingers is about 14 cm. For 3mm glass sphere size, h_{0c} is 1.1cm and ζ (t = 17sec) is about 12cm. Our experiment for regularly packed porous media with same sized glass beads revealed that h_{0c} ranged from 0.1cm to o.42cm (Ueno, 2003). The finger patterns in all the three cases are almost similar. Although more than one finger appeared in the beginning of the experiments, only one finger reached the bottom of the box in each case. The other branched fingers were not as distinct and significant compared to the stem finger. Contrary to our observations, more than one finger appeared simultaneously and continued up to the bottom, as was observed by Zhang and Smith (2001, 2002). This difference in finger numbers can be attributed to wider lateral dimensions of the porous model itself in their experiment. Zhang and Smith used a wider transparent glass box in dimension (0.5H×0.6W×0.01D-m) than that of in our experiment (sees **Fig. 2**). Another important difference between these two studies is the finger propagation velocity. Finger travel time in Zhang and Smith is somewhat longer (4 to 10minutes in travel time) mainly due to smaller glass bead diameter (mean particle diameter varied between 0.32 and 1.36mm).

Experimental correlations between vertical finger length ζ and elapsed time t for the three cases are shown in **Fig. 5**. The vertical distance traversed by the fingers is almost linear for each porous medium type. The slopes of the fitted lines based on two runs data in those correlations represent average vertical velocities of the fingers. Progressive velocities corresponding to 1-mm, 2-mm and 3-mm glass sphere sizes are 0.19, 0.37, and 0.59 cm/s, respectively. As predicted, the average vertical finger velocity increased with the pore size. Thus, these observations disclosed functional relationships among average velocity of the fingers and pore space in the porous media.

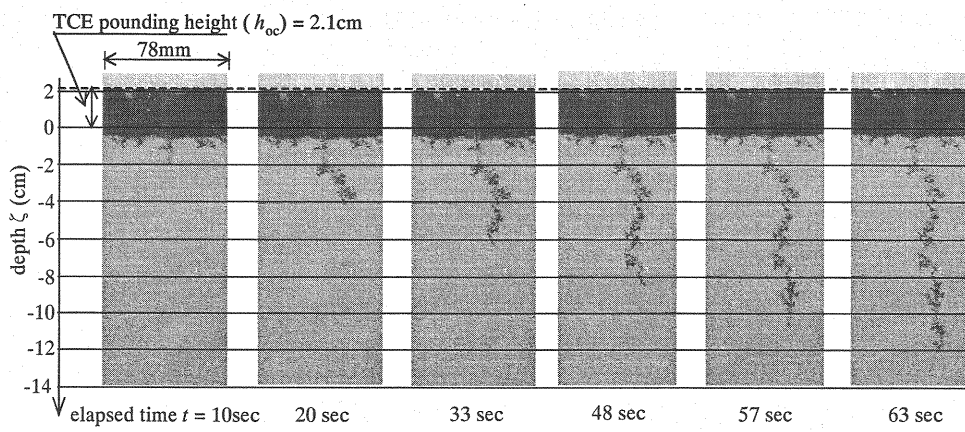

Fig. 3 TCE fingering through a water-saturated porous medium with 1-mm glass sphere size

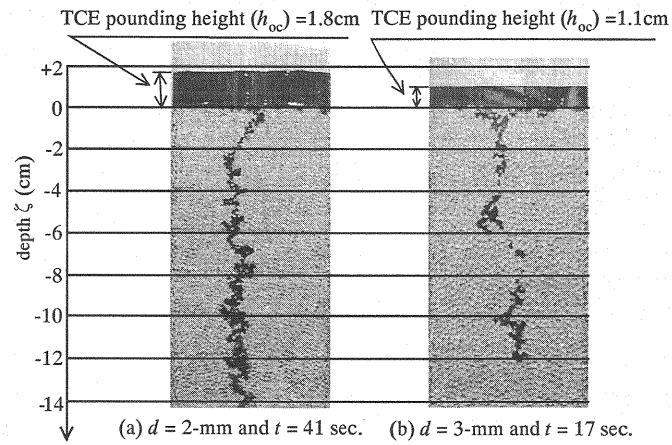

Fig. 4 TCE fingering through water-saturated porous medium with 2 and 3-mm glass sphere sizes

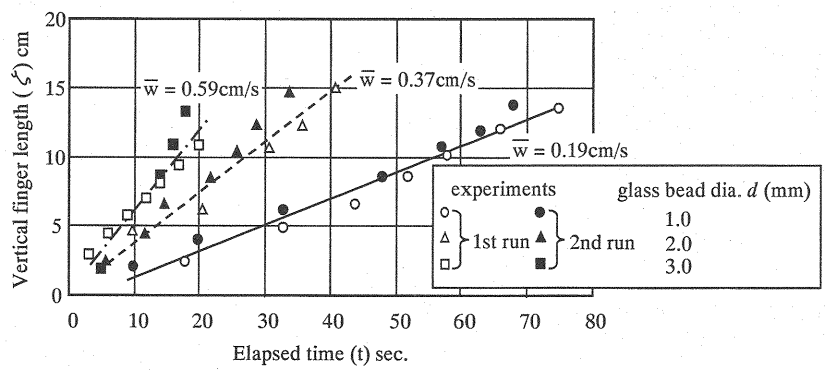

Fig. 5 Finger growth and its average velocity

RESULTS AND DISCUSSION

Formulation for DNAPL Finger Length

A conceptual schematic diagram of TCE fingering through a water-saturated box, as mentioned previously is shown in **Fig. 6**. The winding path is assumed to consist of small path elements, and let us consider an infinitesimal element $d\zeta_s$ of the finger propagating to downwards with intrinsic velocity w_s. Then, the vertical component of the finger velocity is given by $w = w_s \sin\theta_i$. Similarly, $\zeta = \zeta_s \sin\theta_i$ represents the vertical finger length, where ζ_s: the actual finger length at the time considered. TCE, in such a case, moves along a tortuous path through the pores with deviation angel θ_i, and the finger diameter δ_f on many travel path elements is considered to be constant throughout its length (Zhang and Smith, 2001).

By applying Darcy's law for an infinitesimal finger element $d\zeta$ within a small time interval Δt, vertical finger velocity w can be expressed by the following equation:

$$w = kk_r \frac{\left(\zeta + h_{oc} + \zeta_c\right)}{\zeta} \tag{1}$$

where, k: invasion permeability (Darcy's) of DNAPL, k_r: invasion factor related to density difference between DNAPL and pore water, and irregularity of finger, h_{oc}: DNAPL pounding depth at the top of the box, and ζ_c: capillary pressure head of water and DNAPL at the point of consideration in the finger. By applying one-dimensional mass balance for the infinitesimal DNAPL finger along vertical (**Fig. 6**), we get, $d\zeta \sin\theta_i \times 1 \times n_e = w \sin\theta_i \times dt$ for unit cross sectional area of finger. The vertical component of the finger propagation velocity is given by rearranging the mass balance equation as:

$$w = n_e \frac{d\zeta}{dt} \tag{2}$$

where, n_e: effective porosity occupied by DNAPL.
By combining equations (1) and (2), we can obtain a basic equation for DNAPL finger elongation as:

$$kk_r \frac{\left(\zeta + h_{oc} + \zeta_c\right)}{\zeta} = n_e \frac{d\zeta}{dt} \tag{3}$$

Integration of equation (3) gives the following:

$$\int \left(\frac{\zeta}{\zeta + h_{oc} + \zeta_c} \right) d\zeta = \int \frac{kk_r}{n_e} dt + C$$

The constant of integration is evaluated with the condition $\zeta = 0$ for $t = 0$ as,

$$C = -\left(\zeta_c + h_{oc}\right) \ell og \left|\zeta_c + h_{oc}\right|$$

Then, the final equation for finger length is give by,

$$\zeta + \left(\zeta_c + h_{oc}\right) \ell og \frac{\left(\zeta_c + h_{oc}\right)}{\left\{\zeta + \left(\zeta_c + h_{oc}\right)\right\}} = \frac{kk_r}{n_e} t \tag{4}$$

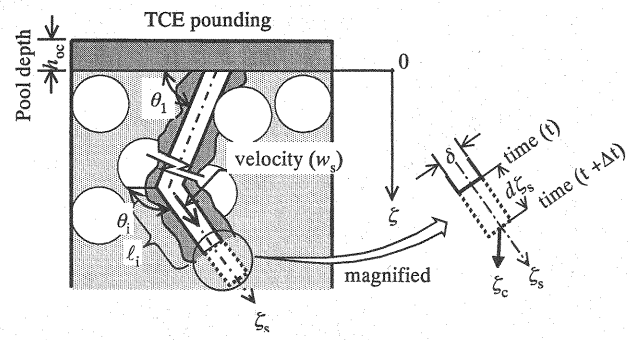

F ig. 6 A conceptual diagram of TCE fingering through a water-saturated porous medium

Table. 2 Parameter values used in calculations

properties of porous medium		TCE ponding depth	effective porosity	invasion factor
glass sphere diameter d (mm)	permeability coefficient k (cm/s)	h_{oc} (cm)	n_e	k_r
1.0	6.1	2.1	0.04	0.001~0.002
			0.05	
2.0	23.4	1.8	0.04	0.0005 ~0.001
			0.05	
3.0	93.2	1.1	0.04	0.0002 ~0.0003
			0.05	

Porous Medium Characteristics and DNAPL Fingering

Equation (4) expresses a functional relationship between finger length and elapsed time. But, the calculation of $\zeta(t)$ is not possible unless the values of ζ_c and some parameters k, k_r and n_e are known. For example, values of permeability k, effective porosity n_e, and invasion factor k_r, and capillary pressure head ζ_c are required for evaluating the relationship. In this study, suitable values of these coefficients are estimated for the cases with three kind sizes of glass sphere (d = 1, 2 and 3-mm). Darcy's permeability of the porous media k is determined by using Kozeny-Carman's empirical equation as:

$$k = d_m^2 g n^3 / 180\nu\left(1-n^2\right) \qquad (5)$$

where, d_m: mean particle size, n: porosity of the medium, ν: kinematic viscosity of the fluid, and g: gravitational acceleration. Other coefficients are determined by comparing theoretical correlations with experimental ones. The values of the coefficients employed in the calculations are shown in **Table 2.**

The correlations of vertical finger length and fingering path lengths ζ with elapsed time t in a water-saturated porous medium model consisting of 1-mm diameter glass spheres and using equation (4) are presented in **Figs. 7**. The experimental results are denoted with circles on theoretical ζ - t curves in different n_e and k_r values. TCE finger velocity ($d\zeta/dt$) increased with decreasing effective porosity, in general, for the same value of invasion factor, as seen in **Fig. 7**. The velocity increased with invasion factor k_r also, as observed in the figure. The experimental results show

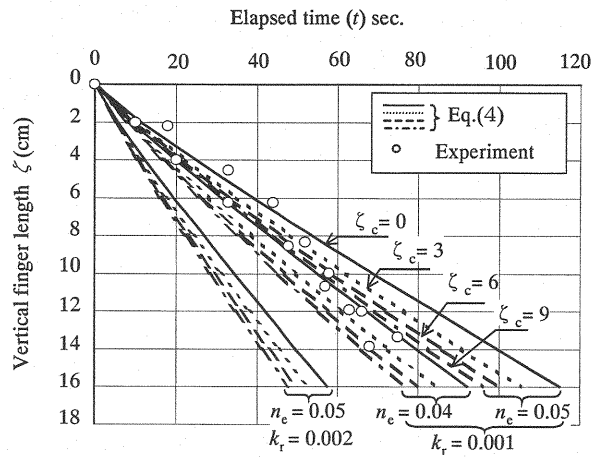

Fig. 7 Relationship between ζ and t for glass sphere diameter d = 1 mm

Table. 3 Inversely identified values of n_e and k_r

parameters	finger length along	glass sphere diameter (d)		
		1.0 mm	2.0 mm	3.0 mm
effective porosity(n_e)	vertical	0.04 ~ 0.05	0.04 ~ 0.05	0.04 ~ 0.05
invasion factor (k_r)	vertical	0.001	0.0005	0.0002 ~ 0.0003

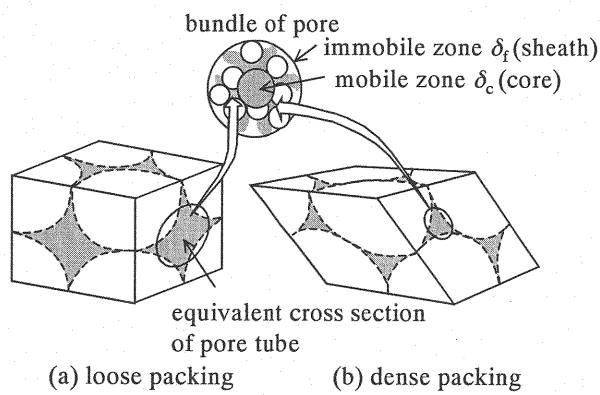

Fig. 8 Unit rhombohedron formed by passing planes through the centers of eight contiguous spheres

that effective porosity n_e varied from 0.04 to 0.05, and invasion factor k_r was 0.001 in the case of vertical finger length (see **Fig. 7**). Similar correlations of finger lengths with time are calculated and compared with the experimental data for two other glass sphere sizes (d = 2 and 3-mm) in the porous media. The theoretical correlations of finger length ζ and with elapsed time t are distinct for capillary pressure values ζ_c from 0 to 9cm. However, the unique value of capillary pressure head ζ_c was not

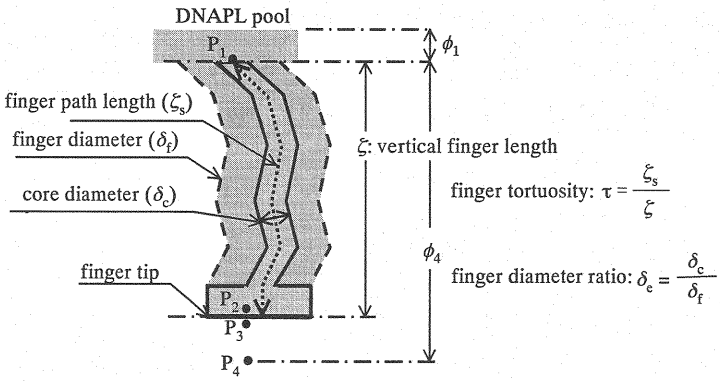

Fig. 9 Mobile-immobile-zone (MIZ) model for DNAPL fingering (Zhang and Smith, 2001)

determined, as can be seen in **Figs. 7**. The estimated values of effective porosity and invasion factor for the three experimental cases are summarized in **Table 3**.

There are two extreme packing structures of an ideal porous medium composed of spherical glass spheres. They are loose and dense packing, as shown in **Fig. 8** (a), (b) (Slichter, 1899). In random packing of spheres, the bulk (or geometrical) porosity n of the medium varies between 0.112 and 0.215. In general, an effective porosity n_e value is smaller than the corresponding bulk porosity. The effective porosity in the experiments discussed in the present study ranged from 0.04 to 0.05 for the three kind of glass sphere (d = 1, 2 and 3-mm). A TCE finger penetrating through a water-saturated porous medium is conceptualized as a tube with constant diameter δ (Zhang and Smith, 2001). The cross-sectional area of the tube is expected to be the same as that of the pore through which the finger passes in loosely and densely packed porous medium models. Then, the tube diameters in dense and loose packing cases are given by $\delta = \{(2\times3^{1/2}\text{-}\pi)\mathrm{d}/2\}^{1/2}$ and $\delta = \{(4\text{-}\pi)\mathrm{d}/\pi\}^{1/2}$ on a closed cut face, respectively (see **Fig. 9**). The values of δ in the present experiments with 1, 2 and 3-mm glass sphere sizes are varied from 0.127 to 0.165, 0.180 to 0.234 and 0.220 to 0.287 mm, respectively. Similarly, the diameter ratios of the TCE finger δ_e (= δ_c/δ_f, δ_c: finger core diameter, δ_f: finger diameter, see **Fig. 9**), which will be discussed in the next section corresponding to the three kinds of glass sphere are δ_e = 0.40, 0.30, and 0.20. It was observed that the finger core diameter δ_c had almost the same values for three kinds of glass media if the equivalent diameter of pore tube as a bundle of pore tubes would be assumed to be equal to those of Zhang and Smith's δ_c.

Mobile-Immobile-Zone (MIZ) Model

Zhang Z. F. and Smith J. E. (2001) proposed a mobile-immobile-zone (MIZ) model to describe DNAPL finger structure and motion in water-saturated porous media. A finger is conceptualized as two circular coaxial tubes. The space between the tubes represents the DNAPL immobile zone or sheath, and the mobile zone or core with tube shaped cross section. However, there is no distinction between these two regions at the tip of the finger since all the DNAPL is mobile. The schematic diagram of a finger and the notations used in the MIZ model are shown in **Fig. 9**. A detailed explanation of the model is available in Zhang and Smith (2001).

They proposed a mathematical equation to express vertical finger velocity based on the MIZ model as:

$$w = \left(\frac{\delta_e}{\tau}\right)^2 \frac{KK_{rd}}{\theta_d \mu_d}\left[g\left(\rho_d - \rho_w\right) + \frac{\left(\phi_1 - \phi_4 - p_c\right) - \varepsilon}{\zeta_s}\right],\ \rho_d > \rho_w \qquad (6)$$

Table. 4 Parameter values used in MIZ model

porous medium model		TCE		water	DNAPL content by volume within finger	relative intrinsic permeability of DNAPL
glass sphere diameter d (m)	intrinsic permeability K (m^2)	density ρ_d (kg/m^3)	viscosity μ_d (Pa.sec)	density ρ_w (kg/m^3)	θ_d	K_{rd}
0.001	2.405×10^{-09}	1468.0	5.66E-04	1000.0	0.386	0.4 ~ 0.6
0.002	9.203×10^{-09}				0.381	
0.003	3.626×10^{-08}				0.437	

where, $\delta_e = \delta_c/\delta_f$: diameter ratio of the mobile core to that of the whole finger; K: intrinsic permeability of DNAPL; K_{rd}: relative intrinsic permeability of the DNAPL; τ: finger tortuosity θ_d: volumetric DNAPL content in the finger; μ_d: dynamic viscosity of DNAPL; ρ_d and ρ_w: densities of DNAPL and water, respectively; ϕ_1 and ϕ_4: hydraulic potentials at points P_1 and P_4, respectively, in **Fig. 9**; p_c: capillary pressure across DNAPL-water interface at the finger tip; ε: hydraulic potential difference between the points P_3 and P_4; ζ_s: actual finger length and ζ: vertical finger length. Point P_1 indicates a point at the top of a finger, point P_2, a tip point of finger, point P_3, outside of P_2, and point P_4, a point on boundary.

They defined finger tortuosity τ as the ratio of actual finger length ζ_s to vertical projection ζ or actual finger velocity w_s to its vertical component w. The term ε/ζ_s is very small and it further decreases with increasing finger length. Similarly, the effect of pounded DNAPL and finger induced flow approach to zero with increasing finger length. Therefore, they neglected the term $(\phi_1 - \phi_4 - p_c)/\zeta_s$ in equation (6). They finally obtained an expression for evaluating relative finger diameter size δ_e as:

$$\delta_e = \tau \left[\frac{w\theta_d \mu_d}{KK_{rd} g\left(\rho_d - \rho_w\right)} \right]^{1/2}, \rho_d > \rho_w \qquad (7)$$

Identification of Relative Finger Diameter and DNAPL Mobility

The relative diameter of the mobile core of TCE fingers in the present experiments was evaluated using equation (7). The parameter values adopted in the calculations are shown in **Table 4**. The intrinsic permeability values for the three porous media in this study were obtained from Kozeny-Carman's empirical equation. TCE content θ_d was calculated using the relation: $\theta_d = n - \theta_{rw}$, where n: measured porosity of the medium (refer to **Table 1**) and θ_{rw}: residual water in the pores after TCE invasion. Zhang and Smith (2001) determined the value of θ_{rw} as 0.1 from moisture characteristic curve for PCE invasion through water-saturated media with glass sphere size varying from 0.32 to1.4mm. We used the same value in this study since the porous media characteristics were almost similar to those observed by Zhang and Smith. The relative intrinsic permeability value for TCE was identified to be between 0.4 and 0.5, which was also adopted from Zhang and Smith (2001). The averaged values of the relative core diameters were identified as 0.40, 0.30 and 0.20 for porous media with 1, 2 and 3-mm glass sphere sizes, respectively, in our study.

DNAPL finger Reynolds number Re is defined as dw/ν_d here, where d: glass sphere diameter employed in the porous media, w: vertical component of finger velocity and ν_d: kinematic viscosity of DNAPL. The finger Reynolds number is a ratio of inertial and viscous forces closely related to fingering. Thus, bigger Re value signifies increased flow instabilities and faster DNAPL movement. A correlation between δ_e and Re for TCE fingers for relative permeability value of $K_{rd} = 0.5$ is presented

in **Fig. 10**. This finding provides evidence that the diameter ratio decreased with increasing Reynolds number. Also, the finger Reynolds number increased with pore size of the porous media. Higher values

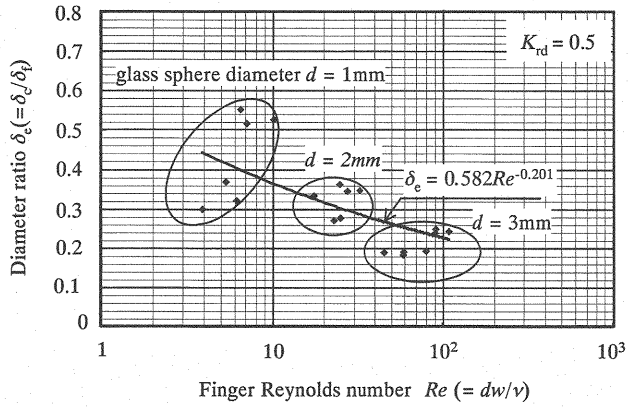

Fig. 10 Relationship between finger Reynolds number (Re) and diameter ratio (δ_e)

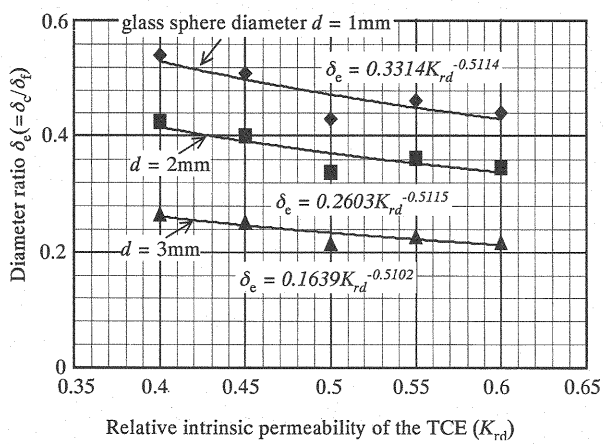

Fig. 11 Relationship between relative intrinsic permeability of TCE (K_{rd}) and finger diameter ratio (δ_e)

of Reynolds number means bigger pore size and vertical finger velocity. Thus, it appears that the diameter of the mobile core within a DNAPL finger decreases with increasing pore size and finger velocity. Conversely, a big fraction of DNAPL is mobile within a finger for smaller pore size and vertical finger velocity. However, as aforementioned, the core diameter δ_c remained almost unchanged in all the experiments. Therefore, this clearly suggests that the variation in finger diameter ratio $\delta_e = \delta_c / \delta_f$ is greatly affected by immobile diameter δ_f (sheath) rather than the pore size and finger Reynolds number. The immobile zone thickness δ_f increased with increasing finger velocity. An experimental correlation between δ_e and Re in this study is expressed as:

$$\delta_e = a\left(Re\right)^{-b} \tag{8}$$

where, the constant "a" and exponent "b" have 0.582 and 0.201 values, respectively. The relative diameter of the mobile core δ_e and finger Reynolds number in this case varied from 0.44 to 0.23, and

from 4.0 to 110.0, respectively. It says that the DNAPL core size δ_c can not be determined if the pore size δ and effective porosity occupied by DNAPL n_e are estimated.

Referring to K_{rd} in Table 4, correlations between relative finger diameter δ_e and relative intrinsic permeability K_{rd}, using Eq. (7) proposed by Zhang and Smith, for the three kind sizes of glass sphere are shown in **Fig. 11**. The diameter ratio gradually decreased with increasing relative intrinsic permeability. The tendency of the relationship seemed similar to the three kinds of glass sphere. A clear difference among them is the decrease of diameter ratio with increasing pore size. Thus, a comparison of these three cases in **Fig. 11** also reveals that the overall finger diameter increased with pore size. Therefore, it is apparent that size of the immobile zone δ_f increased with finger Reynolds number Re and relative intrinsic permeability K_{rd}, which may suggest longer DNAPL persistence in the saturated pore space.

CONCLUSION

TCE fingering through water-saturated porous medium models, which were prepared with randomly packed uniform size glass spheres in a transparent glass box, was visualized in laboratory scale experiments. Once fingering was initiated, TCE fingers grew almost linearly with time, which was similar to the observations made by Zhang and Smith (2001 and 2002). A basic mathematical model relating finger length and properties of porous medium and TCE under constant pounding boundary condition was developed. TCE fingering characteristics were interpreted by using the experimental data and the basic equation. The values of effective porosity n_e varied from 4.0×10^{-2} to 5.0×10^{-2} irrespective of the glass sphere size in the porous media. However, invasion factor k_r increased with increasing pore size in the media, and the values were between 2.0×10^{-4} and 1.0×10^{-3}.

TCE mobility and other fingering characteristics through the water-saturated porous media were examined by means of the MIZ model proposed by Zhang and Smith (2001). The relative core diameters of the fingers δ_c for three kind sizes of glass sphere ranged between 0.20 and 0.40. The results showed that mobile core diameters δ_c of the fingers were almost the same while size of immobile zone δ_f increased with finger Reynolds number and relative intrinsic permeability. These findings suggested that less mobile TCE (within sheath) occupied wider pore space in the porous media. The finger Reynolds number in our experimental study covered between 4.0 and 110.0. The results obtained from this study will be useful in providing a new approach to deal with the fingering phenomenon.

ACKNOWLEDGEMENTS

This work has been supported by Grants-in-Aid (Representative person: Dr. Kuniaki Sato, Professor of Geosphere Research Institute, Saitama University) for Scientific Research System, (C)-(1), No.14550539 on "development of integrated numerical method for predicting soil and groundwater pollution based on atmosphere linked model" in 2002 and 2003 fiscal years. The authors are grateful to president, Motoyuki Ono, of Japan Society for the Promotion of Science (JSPS).

REFERENCES

1. Bear J. (1972): *Dynamics of Fluids in Porous Media*, American Elsevier, pp.165-167.
2. Glass R.J., Conrad S.H. and Peplinski W. (2000): Gravity-destabilized phase invasion in macroheterogeneous porous media: Experimental observations of invasion dynamics and scale analysis. *Water Resources Research*, Vol. 36, No. 11, pp. 3121-3137.
3. Held R.J. and Illangasekare T.H. (1995): Fingering of dense non-aqueous phase liquids in porous media. 2: Analysis and classification. *Water Resources Research*, Vol. 31, No. 5, pp. 1223-1231.
4. Held, R.J. and Illangasekare, T.H. (1995): Fingering of dense non-aqueous phase liquids in porous media: 1. Experimental investigation, *Water Resources Research*, Vol.31, No. 5, pp.1213-1222.

5. Kueper, B.H. and Frind, E.O. (1988): An overview of immiscible fingering in porous media, *Journal of Contaminant Hydrology*, Vol.2, pp. 95-110.
6. Mercer J.W. and Cohen R.M. (1990): A review of immiscible fluids in the subsurface: properties, models, characterization and remediation. *Journal of Contaminant Hydrology*, Vol. 6, pp. 107-163.
7. Oostrom M., Hofstee C., Walker R.C. and Dane J.H. (1999): Movement and remediation of trichloroethylene in a saturated heterogeneous porous medium. 1: Spill behavior and initial dissolution. *Journal of Contaminant Hydrology*, Vol. 37, pp. 159-178.
8. Pankow J.F. and Cherry J.A. (1996): *Dense Chlorinated Solvents and other DNAPLs in Groundwater*. Waterloo Press, Ontario, Canada.
9. Salah J., Paul M., Oliver R. and Gerhard S. (2001): Large scale experiment on transport of trichloroethylene in a controlled aquifer. *Transport in Porous Media*, Vol. 44, pp. 145-163.
10. Slichter C. (1899): Theoretical investigation of the motions of ground waters. *United State Geological Survey*, pp. 301-323.
11. Smith J.E. and Zhang Z.F. (2001): Determining effective interfacial tension and predicting finger spacing for DNAPL penetration into water-saturated porous media. *Journal of Contaminant Hydrology*, Vol. 48, pp. 167-183.
12. Ueno T. (2003): Dynamic mechanism on gravitational dispersion on dense non-aqueous phase liquids in porous medium model. *Doctor thesis of Saitama University*, pp. 23-47
13. Zhang Y., Shariati M. and Yortsos Y.C. (2000): The spreading of immiscible fluids in porous media under the influence of gravity. *Transport in Porous Media*, Vol. 38, pp. 117-140.
14. Zhang, Z.F. and Smith, J.E. (2001): The velocity of DNAPL fingering in water-saturated porous media: laboratory experiments and a mobile-immobile-zone model, *Journal of Contaminant Hydrology*, Vol. 49, pp. 335-353.
15. Zhang, Z.F. and Smith, J.E. (2002): Visualization of DNAPL fingering processes and mechanisms in water-saturated porous media, *Transport in Porous Media*, Vol. 48, pp. 41-59.

(Received June 25, 2003 ; revised September 29, 2003)